

DNAX-activating protein 10 co-stimulation enhances the anti-tumor efficacy of chimeric antigen receptor T cells

Ruocong Zhao^{a,b,c}, Lin Cheng^{b,a,b}, Zhiwu Jiang^{a,b}, Xinru Wei^{a,b}, Baiheng Li^{a,b}, Qiting Wu^{a,b}, Suna Wang^{a,b}, Simiao Lin^{a,b}, Youguo Long^{a,b}, Xuchao Zhang^d, Yilong Wu^d, Xin Du^e, Duanqing Pei^{a,b}, Pentao Liu^{b,f}, Yangqiu Li^{b,g}, Shuzhong Cui^h, Yao Yao^{a,b}, and Peng Li^{a,b,h}

^aKey Laboratory of Regenerative Biology, South China Institute for Stem Cell Biology and Regenerative Medicine, Guangzhou Institutes of Biomedicine and Health, Chinese Academy of Sciences, Guangzhou, China; ^bGuangdong Provincial Key Laboratory of Stem Cell and Regenerative Medicine, South China Institute for Stem Cell Biology and Regenerative Medicine, Guangzhou Institutes of Biomedicine and Health, Chinese Academy of Sciences, Guangzhou, China; ^cUniversity of Chinese Academy of Sciences, Beijing, China; ^dGuangdong Lung Cancer Institute, Medical Research Center, Guangdong General Hospital, Guangdong Academy of Medical Sciences, Guangzhou, China; ^eDepartment of Hematology, Guangdong General Hospital, Guangdong Academy of Medical Sciences, Guangzhou, China; ^fSchool of Biomedical Sciences, Li Ka Shing Faculty of Medicine, Stem Cell and Regenerative Medicine Centre, University of Hong Kong, Hong Kong, China; ^gInstitute of Hematology, Medical College, Jinan University, Guangzhou, China; ^hAffiliated Cancer Hospital & Institute of Guangzhou Medical University, Guangzhou, China

ABSTRACT

Chimeric antigen receptor (CAR) T cell immunotherapies have shown remarkable efficacy in treating multiple types of hematological malignancies but are not sufficiently effective at treating solid tumors. NKG2D is a strong activating receptor for NK cells and a co-stimulatory receptor for T cells. NKG2D signal transduction depends on DNAX-activating protein 10 (DAP10). Here, we introduced the cytoplasmic domain of DAP10 into the second-generation CARs M28z and G28z to generate M28z10 and G28z10, which target mesothelin (MSLN) and glypican 3 (GPC3), respectively. T cells expressing M28z10 or G28z10 showed enhanced and prolonged effector function against MSLN+ lung cancer or GPC3+ hepatocellular carcinoma cell lines in culture and secreted elevated levels of cytokines, including IL-2, IFN- γ , granzyme B, and GM-CSF. In addition, M28z10 CAR-T cells showed greater anti-tumor activity than those expressing M28z in both A549 cell line xenografts and human lung cancer patient-derived xenografts (PDX). Similarly, G28z10 exhibited higher efficacy in causing tumor regression than did G28z in hepatocellular carcinoma PDX. Therefore, our results show that DAP10 signaling contributes to the function of CAR-T cells in both lung cancer and hepatocellular carcinoma and can enhance the efficacy of CAR-T cells.

ARTICLE HISTORY

Received 8 March 2018
Revised 19 July 2018
Accepted 2 August 2018

KEYWORDS

CAR-T; NKG2D; DAP10; mesothelin; glypican 3

Introduction

In recent years, the clinical application of chimeric antigen receptor T cells (CAR-T) has achieved considerable success in the treatment of hematological malignancies, including CD19-positive B cell acute leukemia.^{1–5} CARs contain an extracellular ScFv fragment recognizing tumor-associated antigens (TAAs), the CD3z intracellular T cell-activating domain and co-stimulatory domains such as those derived from CD28 and 4-1BB. Upon binding of target antigens by ScFv, the signaling domains are activated, leading to target cell killing and CAR-T cell proliferatio.^{6–8} The first-generation CAR utilized only CD3z to activate T cells without incorporating a co-stimulatory domain, the in vivo anti-tumor efficacy of these cells is poor.⁹ Second-generation CAR-T cells, which generally utilize CD28 or 4-1BB as a co-stimulatory signal, have shown surprising efficacy in leukemia patient.^{2,6,10} Nonetheless, the efficacy of CAR-T cells against solid tumors remains poor and uncertain, perhaps due to factors that suppress T cell responses in the tumor microenvironment.^{11–13}

Studies have shown improved anti-tumor activity by simultaneously incorporating CD28 and 4-1BB cytoplasmic domains into a CAR vector to construct a third-generation CA.^{14,15} In addition to CD28 and 4-1BB, other co-stimulatory molecules, such as ICOS, OX-40, CD40, and CD27, have been tested in multiple pre-clinical model.^{16–19} Previously, we determined that co-stimulation of toll-like receptor 2 can potentiate the anti-tumor efficacy of CAR-T cell.²⁰ Together, these findings demonstrate the importance of optimizing the co-stimulatory molecules in CAR-T cells.

Natural killer (NK) group 2 member D (NKG2D) is a strong activating receptor for both human and murine NK cells. In addition, NKG2D is expressed by CD8 + T cells and reportedly serves as a co-stimulatory receptor for CD8 + T cells. The membrane localization and signal transduction of NKG2D in T cells depend on another membrane protein, DNAX-activating protein 10 (DAP10). DAP10 contains a YxxM signaling motif, which may activate phosphatidylinositol 3-kinase-dependent signaling pathway.^{21,22} Despite the roles of NKG2D and DAP10 signaling on T cells have been extensively studied,^{23,24} the effect of DAP10 activation in the

second-generation CAR-T cells, which generally utilize a CD28 or 4-1BB co-stimulatory domain, remains unknown. We hypothesized that DAP10 activation can improve the anti-tumor activity of second-generation CAR-T cells based on previous reports. To test this hypothesis, we generated anti-mesothelin (MSLN) and anti-glypican 3 (GPC3) CAR vectors containing the DAP10 cytoplasmic domain, CD28 and 4-1BB. We compared the function of CAR-T cells with or without the DAP10 cytoplasmic domain using in vitro functional assays and in vivo xenograft mouse models. Our results reveal that DAP10 incorporation enhances the effector function and anti-tumor capacity of second-generation CAR-T cells in vitro and in vivo.

Results

DAP10 incorporation in second-generation anti-msln cars enhanced anti-tumor activity in vitro

We generated second-generation anti-MSLN CAR-T cells with a CD3z activating domain and a CD28 cytoplasmic domain (M28z) as previously reported.²⁰ To confirm the expression of NKG2D and DAP10 in CAR-T cells, we detected NKG2D expression on in vitro-expanded CAR-T cells by FACS, and most of the expression was detected on CD8+ CAR-T cells (Supplementary Figure 1A). DAP10 gene expression in these cells was then confirmed by qRT-PCR (Supplementary Figure 1B). The results show the expression of NKG2D and DAP10 in M28z CAR-T cells.

To stably couple and activate DAP10 signaling with CARs, we constructed vectors containing the DAP10 cytoplasmic domain based on the second-generation CARs M28z and Mbbz, named M28z10 CAR and Mbbz10 CAR, respectively (Figure 1A). We then sought to determine if DAP10 incorporation in the CAR vectors affects the anti-tumor activity of CAR-T cells. We transduced these constructs into primary human T cells and found no difference in transduction efficiency in the M28z and M28z10 groups (Supplementary Figure 2). Then, we tested the in vitro killing capacity of these CAR-T cells. Specifically, GFP, M28z, M28z10, Mbbz, and Mbbz10 T cells were co-cultured with human lung cancer cell lines, including A549GL, H460GL and MSLN-overexpressing H460GL cells, at the indicated effector to target (E:T) ratio for 18 hours, and target cell viability was then determined by measuring luciferase activity with a 450-nm laser in a luminometer. The results showed that the cytotoxicity of M28z10 was greater than that of M28z in A549GL and H460GL MSLN+ target cells, while there was no difference in cytotoxicity against H460GL cells, which do not express MSLN (Figure 1B). To determine the levels of cytokine secretion by these different CAR-T cells, the supernatant of T cells co-cultured with A549GL cells was collected for enzyme-linked immunosorbent assay (ELISA) analysis. The secretion of IL-2, IFN- γ , granzyme B, and GM-CSF was significantly elevated in the M28z10 group compared with the M28z and GFP groups. Similar results were also obtained in Mbbz10 T cells compared with Mbbz and GFP T cells, except for GM-CSF, which was secreted at high levels by the Mbbz group

(Figure 2A). These results show the enhanced capacity for cytokine secretion upon DAP10 incorporation in second-generation CAR-T cells.

DAP10 incorporation in second-generation anti-msln cars enhanced the serial killing activity in vitro

We then sought to determine the serial killing capacity of M28z10 and Mbbz10 T cells by continuously challenging them 3 times with A549GL target cells at 24-hour intervals. GFP, M28z, M28z10, Mbbz, and Mbbz10 T cells were co-cultured with A549GL cells at an E:T ratio of 1:2. After 24 hours, suspended T cells were transferred to another plate, and the remaining adherent cells were assayed for luminescence; Then, the same number of A549GL cells was added to the T cells. Twenty-four hours later, the procedure was repeated. The results showed that during the 3 rounds of killing, the cytotoxicity of all groups of T cells decreased, and M28z10 and Mbbz10 T cells exhibited significantly greater cytotoxicity than GFP, M28z and Mbbz T cells in all 3 rounds of killing (Figure 2B). We also detected IL-2 and granzyme B secretion after the 3rd challenge; at this time point, all groups of T cells showed decreased cytokine secretion, but M28z10 and Mbbz10 T cells retained significantly higher secretion levels than did GFP, M28z and Mbbz T cells (Figure 2C). Flow cytometry analysis of M28z10 and M28z T cells after 3 rounds of A549 target cell stimulation revealed a significant elevation of CD25, CD69 and CD107a expression on the surface of M28z10 T cells, indicating an increased activation state and increased degranulating capacity. A moderate elevation of PD-1 expression was detected, which also suggests enhanced T cell activation (Figure 2D). Taken together, these results show that cytotoxicity, cytokine secretion, and T cell activation are enhanced by DAP10 incorporation into anti-MSLN CARs.

DAP10 incorporation in anti-msln cars enhanced anti-tumor activity in vivo

To test whether DAP10 incorporation enhances the anti-tumor efficacy of CAR-T cells in vivo, we firstly constructed a human lung cancer xenograft mouse model by subcutaneously (s.c.) injecting 5×10^5 A549GL cells into NOD-SCID IL2 γ -/- (NSI) mic.²⁵ After 2 weeks, tumors reached approximately 100 cm³ in size, and 5×10^6 M28z or M28z10 T cells and an equivalent number of GFP T cells were intravenously (i.v.) infused into these mice. Tumor volume was measured every 3 days. On day 39, the mice were sacrificed, and the tumors were dissected (Figure 3A). The results showed that tumor growth was delayed in the M28z10 T cell group compared with both the M28z T cell and GFP T cell groups (Figure 3B); tumor weight was also lower in the M28z10 group (Figure 3C). Immunohistochemistry detection of human CD3 in the tumor tissue sections showed more infiltrated T cells in M28z10 T cells treated mice compared with M28z T cells treated mice (Figure 3D). Taken together, these results indicate that incorporating the DAP10 cytoplasmic domain into

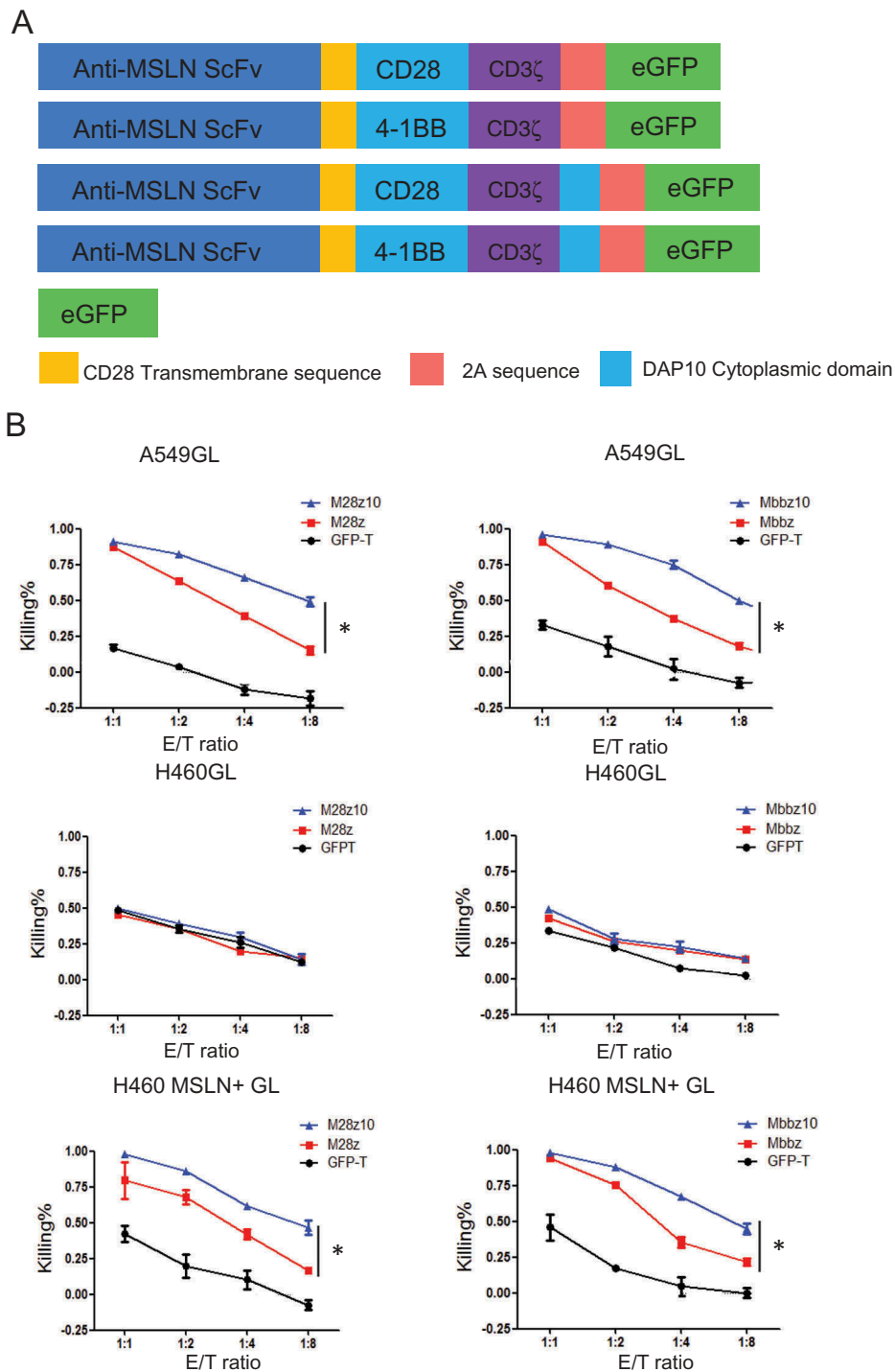


Figure 1. DAP10 incorporation in second-generation anti-mesothelin CARs enhanced cytotoxicity in vitro. (A) Schematic diagram of M28z, Mbbz, M28z10, Mbbz10, and GFP vector construction. (B) Eighteen-hours in vitro killing assay of M28z, M28z10, Mbbz, Mbbz10, and GFP T cells on multiple lung cancer cell lines, including A549GL, H460GL and MSLN+ H460GL cells, at each E/T ratio. * $P < 0.05$, ** $P < 0.01$, and *** $P < 0.001$.

the CAR vector improves the anti-tumor efficacy in NSCLC cell line based tumor model in vivo.

To further test the efficacy of DAP10 activation in CAR-MSLN T cells, we utilized a primary lung cancer sample that expresses the MSLN antigen to construct a patient-derived xenograft mouse model.²⁶ Eighteen days after tumor inoculation, we i.v. infused 5×10^6 M28z or M28z10 T cells or an equivalent number of GFP T cells into these mice, and the CAR-T cell percentage was normalized with untransduced T

cells. Tumor volume was measured every 3 days after infusion, and mice were sacrificed on day 38 (Figure 4A). Tumors were dissected to analyze the volume and weight; tumor samples were collected to detect the persistence of CAR-T cells in these mice by FACS. The results showed that M28z10 T cells delayed primary lung cancer growth, and tumor weight was lower in the M28z10 T cell group than in the M28z and GFP T cell groups (Figure 4B and C). FACS analysis indicated that the percentages of both total T cells

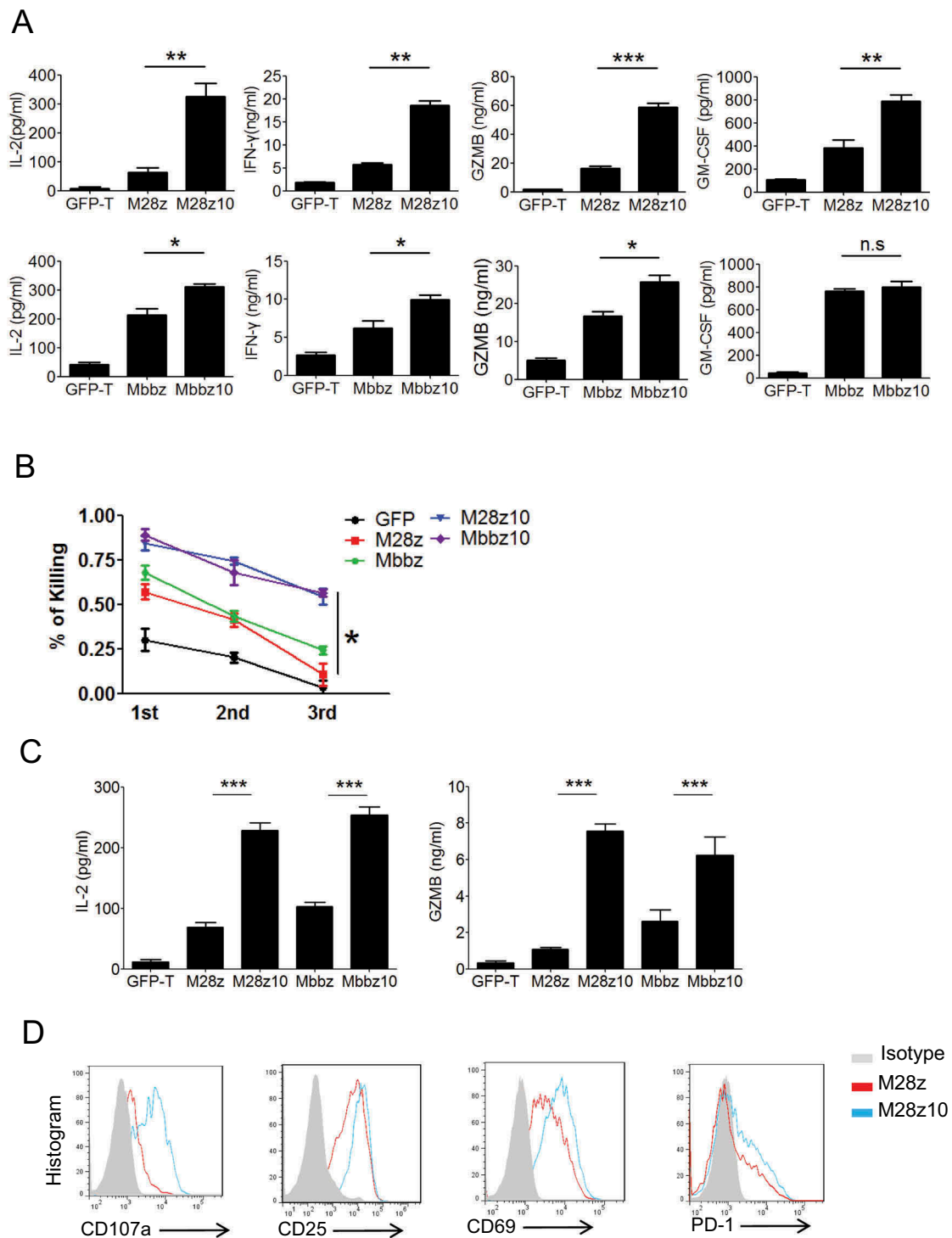


Figure 2. DAP10 incorporation in second-generation anti-mesothelin CARs enhanced cytokine secretion and serial killing activity in vitro. (A) Detection of IL-2, IFN- γ , granzyme B and GM-CSF secretion by M28z, M28z10, Mbbz, Mbbz10, and GFP T cells after co-culture with A549GL cells for 18 hours. (B) Serial killing assay of M28z, Mbbz, M28z10, and GFP T cells against A549GL cells. Specifically, T cells were co-cultured in 3 rounds with A549 cells at an E:T ratio of 1:2, and target cell viability was measured after each killing round. (C) IL-2 and granzyme B secretion by T cells after 3 rounds of killing A549GL cells. (D) Detection of cell surface markers of T cell activation, degranulation, and exhaustion after 3 rounds of killing A549 cells. * $P < 0.05$, ** $P < 0.01$, and *** $P < 0.001$.

and CAR-T cells were elevated in the M28z10 group compared with the M28z group, which showed low persistence in this experiment (Figure 4D and E, Supplementary Figure 3). These results show the improved anti-tumor efficacy of M28z10 T cells with increased accumulation of CAR-T cells in the tumor microenvironment.

DAP10 incorporation in anti-gpc3 cars enhanced anti-tumor activity in vitro and in vivo

GPC3 is a glycoprotein widely expressed on human hepatocellular carcinoma (HCC) cell,^{27,28} and GPC3 has been developed as an antigen in CAR-T therapy for multiple pre-clinical and clinical

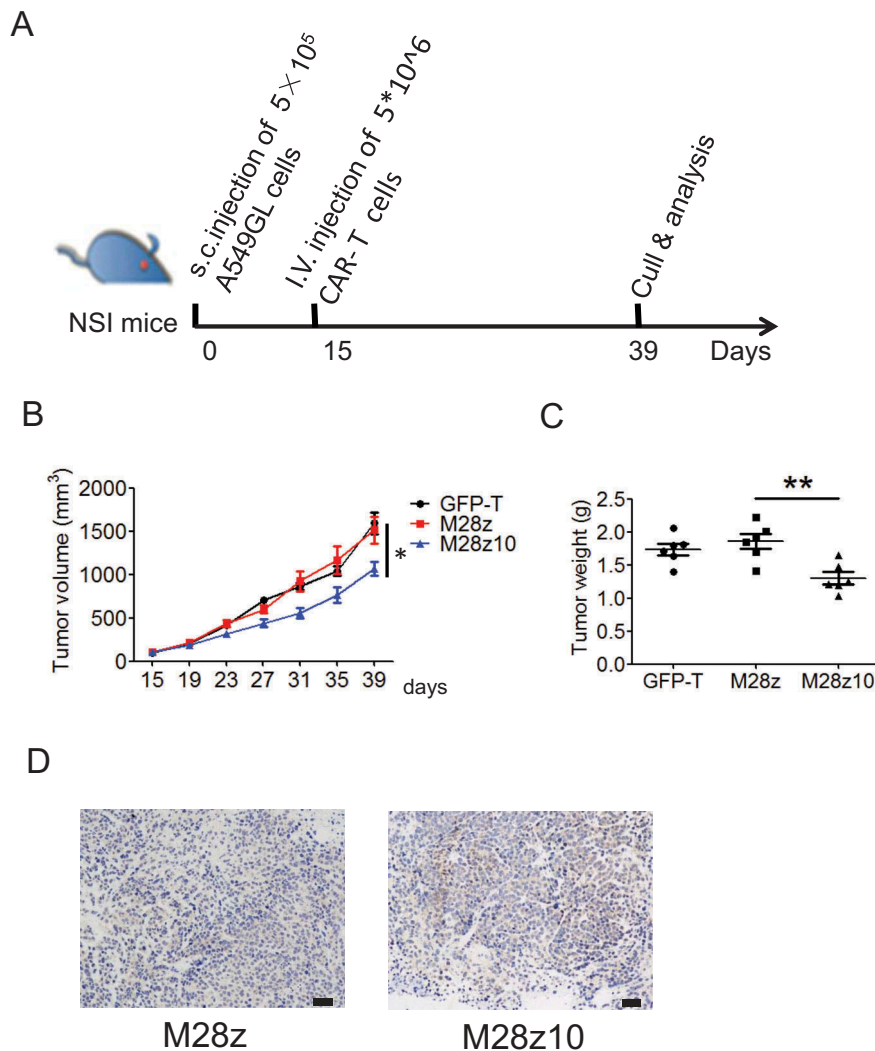


Figure 3. DAP10 incorporation in anti-mesothelin CARs enhanced anti-tumor activity in A549 lung cancer cell xenograft mouse models. (A) Schematic representation of the experiments. (B-C) Tumor volume (B) and weight (C) of A549 mouse xenografts after treatment with GFP, M28z, or M28z10 T cells. (D) CD3 expression in the tumor of M28z and M28z10 T cells treated mice detected by Immunohistochemistry. Scale Bar = 20 μm . Tumor volume = (length \times width²)/2; Error bars denote s.e.m., and the results were compared with an unpaired t-test. * $P < 0.05$, ** $P < 0.01$, and *** $P < 0.001$.

application.^{29,30} To further confirm the effect of DAP10 on second-generation CAR-T cells, we next constructed anti-GPC3 CAR vectors containing the DAP10 cytoplasmic domain at the 3' end of the CAR (Figure 5A). We then assessed the in vitro killing of the human HCC cell lines HepG2GL and HC04GL by GFP, G28z, G28z10, Gbbz and Gbbz10 T cells in co-cultures at the indicated E:T ratio for 18 hours. HepG2GL and HC04GL cells were generated by transducing the human HCC cell lines HepG2 and HC-04 with luciferase-GFP lentivirus as previously reported.³⁰ G28z10 and Gbbz10 T cells exhibited increased cytotoxicity compared with G28z and Gbbz T cells, respectively (Figure 5B). Cytokine assays performed after co-culturing T cells with HepG2GL cells demonstrated increased IL-2, IFN- γ , granzyme B and GM-CSF secretion by G28z10 T cells compared with G28z T cells. IL-2, IFN- γ and granzyme B secretion was increased in the Gbbz10 group compared with the Gbbz group, but GM-CSF secretion by Gbbz and Gbbz10 T cells was similar (Figure 5C).

Next, we tested the anti-tumor efficacy of anti-GPC3 CAR-T cells in a primary HCC xenograft mouse model. Primary HCC samples were s.c. transplanted into NSI mice. After 18 days,

5×10^6 G28z or G28z10 T cells or an equivalent number of GFP T cells were i.v. injected into these mice. Tumor volume was measured every 3 days. Mice were sacrificed 27 days after tumor transplantation (Supplementary Figure 4A). Both G28z and G28z10 T cells significantly suppressed tumor growth and caused regression of these primary HCC tumors, but G28z10 T cells had greater efficiency in evoking HCC tumor regression (Supplementary Figure 4B). These results show that G28z10 T cells are more efficient than G28z T cells at inducing primary HCC regression, suggesting enhanced anti-tumor activity induced by DAP10 activation in T cells.

Synergistic effect of CD28 and DAP10 cytoplasmic domains in promoting the effector function of CAR-T cells

The above data demonstrates the enhanced anti-tumor activities of DAP10 incorporation into the second generation CAR vectors, nonetheless, the function of CAR containing only DAP10 as co-stimulatory signal should also be evaluated to know whether DAP10 can fully co-stimulate CAR-T cells only by itself without

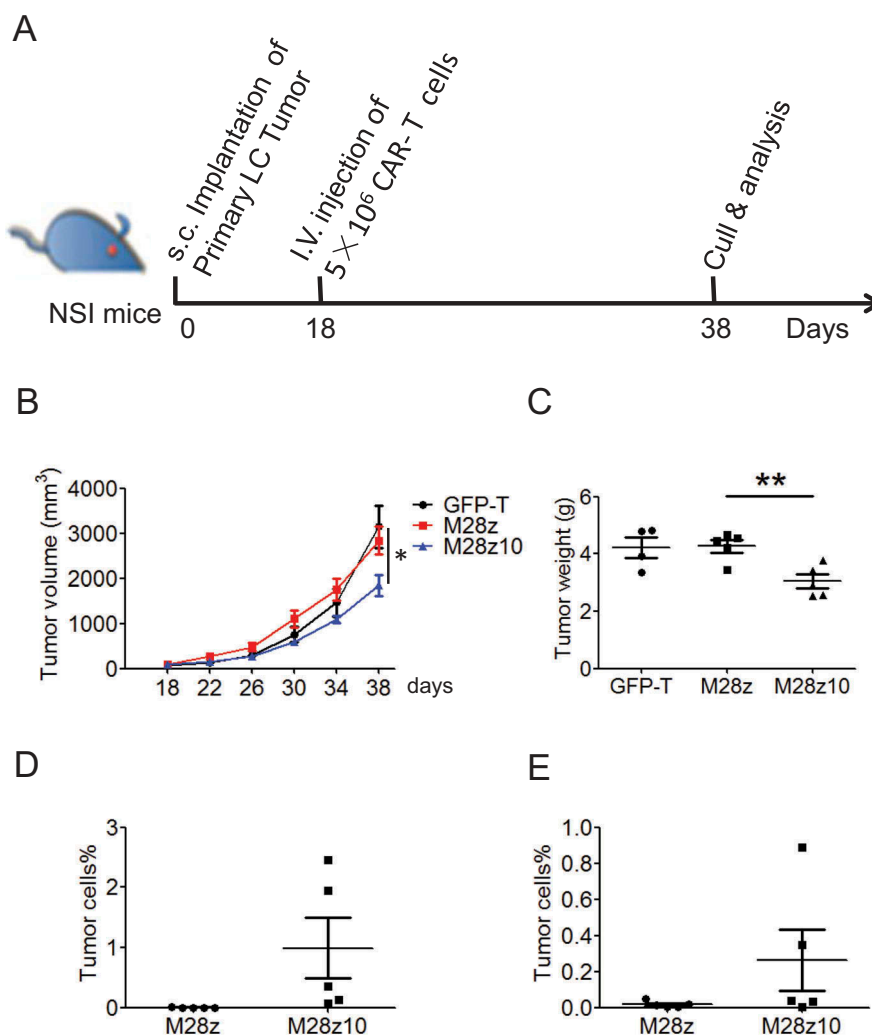


Figure 4. DAP10 incorporation in anti-mesothelin CARs enhanced anti-tumor activity in human primary lung cancer cell xenograft mouse models. (A) Schematic representation of the experiments. (B-C) Tumor volume (B) and weight (C) of primary lung cancer mouse xenografts after treatment with GFP, M28z, or M28z10 T cells. Tumor volume = $(\text{length} \times \text{width}^2)/2$. (C-D) Percentage of total human T cells (C) and CAR-T cells (D) in primary lung cancer tissue. Error bars denote s.e.m., and the results were compared with an unpaired t-test. * $P < 0.05$, ** $P < 0.01$, and *** $P < 0.001$.

the assistance of CD28 or 4-1BB domains. Therefore, we constructed the second generation CAR vector which only utilize DAP10 as co-stimulatory signal (Figure 6A), named Mz10. Then we sought to determine the in vitro functions of Mz10, M28z, and M28z10 T cells in terms of cytotoxicity and cytokine secretion. The results show that the cytotoxicity of Mz10 T cells against A549GL cells is comparable with M28z T cell, and is also significantly lower than M28z10 T cells (Figure 6B). Similar results were obtained from cytokine detection assays, which suggested the similar IL-2 and granzyme B secretion level for Mz10 and M28z T cells, while M28z10 T cells secreted significantly higher level of them (Figure 6C). These data indicate that DAP10 are not able to co-stimulate CAR-T cells to the extent elicited by both CD28 and DAP10. These results also indicate the showed synergistic effect of CD28 and DAP10 in co-stimulating CAR-T cells, as demonstrated by the highest level in both cytotoxicity and cytokine secretion exhibited by M28z10 T cells.

To explore the mechanisms underlying the synergistic effect of CD28 and DAP10, we focused on the two transcription factors, T-bet and Eomesodermin (Eomes), which are master transcriptional regulators in T cells and mediated their effector

function or memory differentiation.^{31,32} We firstly detected the levels of T-bet and Eomes mRNA transcripts in GFP, Mz10, M28z, M28z10 T cells after co-culturing them with A549GL cells at E:T ratio = 2:1 by qRT-PCR. The results show that M28z10 T cells exhibit highest level of T-bet transcripts compared with M10z and M28z T cells, while M10z and M28z show similar level of T-bet transcripts (Figure 6D). To confirm the expression of T-bet at protein level, we performed intracellular flow cytometry staining to detect T-bet expression in the CAR-T cells, the results showed that the percentage of T-bet positive cells is highest in M28z10 group compared with Mz10 and M28z group (Figure 6E).

Discussion

In the present study, we generated 3rd generation CAR-T cells containing the DAP10 cytoplasmic domain and the CD28 or 4-1BB cytoplasmic domain as co-stimulatory signals for T cells. DAP10 incorporation in anti-MSLN and anti-GPC3 CAR-T cells elicited enhanced cytotoxicity and cytokine secretion in vitro. Moreover, anti-tumor activity was improved, as shown by the

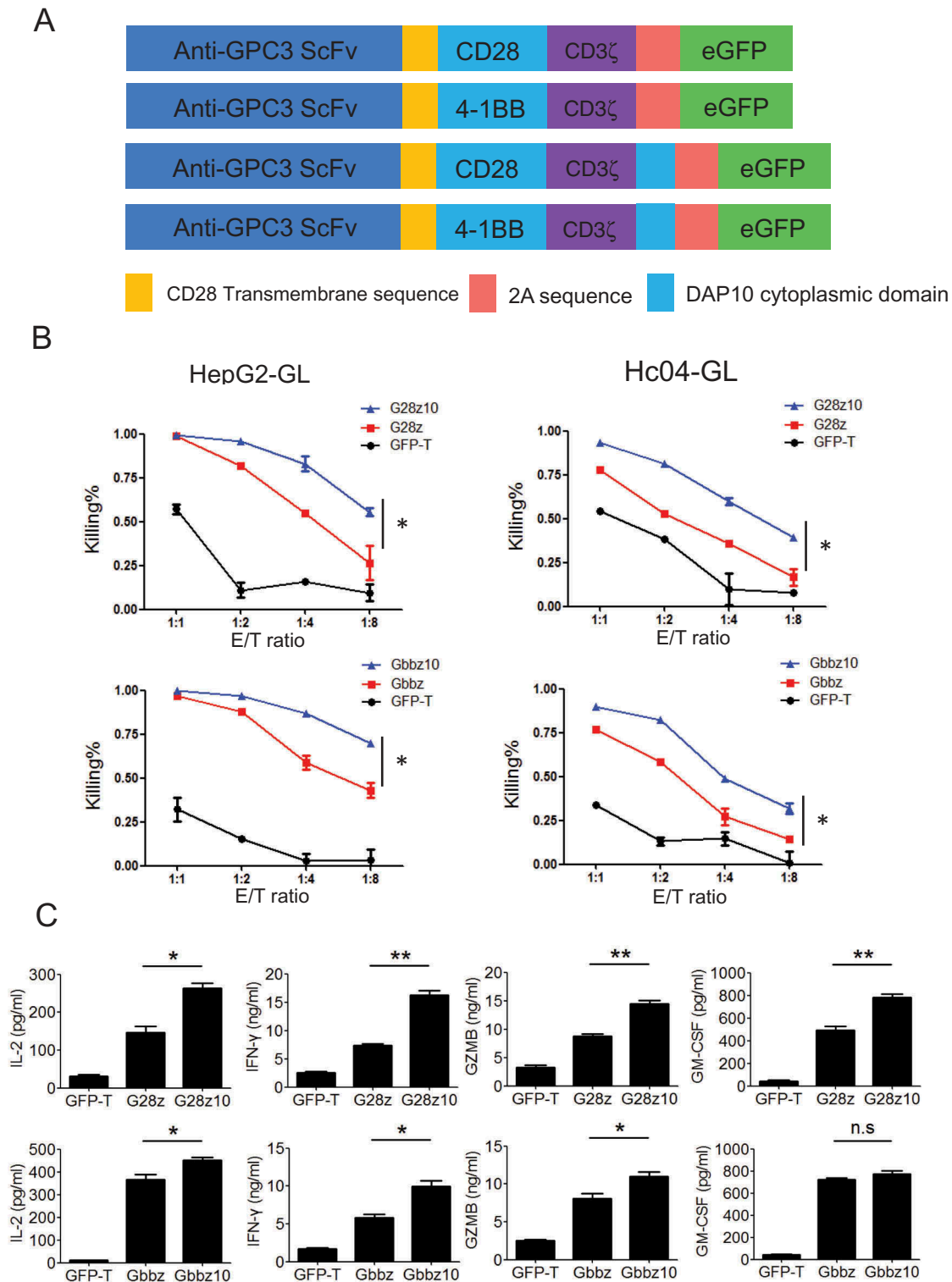


Figure 5. DAP10 incorporation in second-generation anti-glypican 3 CARs enhanced cytotoxicity and cytokine secretion in vitro. (A) Schematic diagram of G28z, Gbbz, G28z10 and Gbbz10 vector construction. (B) Eighteen-hour in vitro killing assay of G28z, G28z10, Gbbz, Gbbz10, and GFP T cells on the human hepatocellular carcinoma cell lines HepG2GL and HC04GL at each E:T ratio. (C) Detection of IL-2, IFN- γ , granzyme B and GM-CSF secretion by G28z, G28z10, Gbbz, Gbbz10, and GFP T cells after co-culture with HepG2GL cells for 18 h. * $P < 0.05$, ** $P < 0.01$, and *** $P < 0.001$.

delayed tumor growth in our xenograft cell line and PDX mouse models. Collectively, our data show the enhancement of anti-tumor capacity by DAP10 incorporation in second-generation CAR-T cells.

Ligand binding to NKG2D activates the signal transducer DAP10 to trigger downstream phosphorylation cascades,

leading to the activation of NK cells or co-stimulation of T cell.^{22,33} Cytokines such as IL-4 and TGF- β derived from the tumor microenvironment can down-regulate NKG2D expression on NK and CD8 + T cells and thereby dampen anti-tumor activity.^{34–36} In contrast, cytokines that function through common γ chain receptors, including IL-2, IL-7,

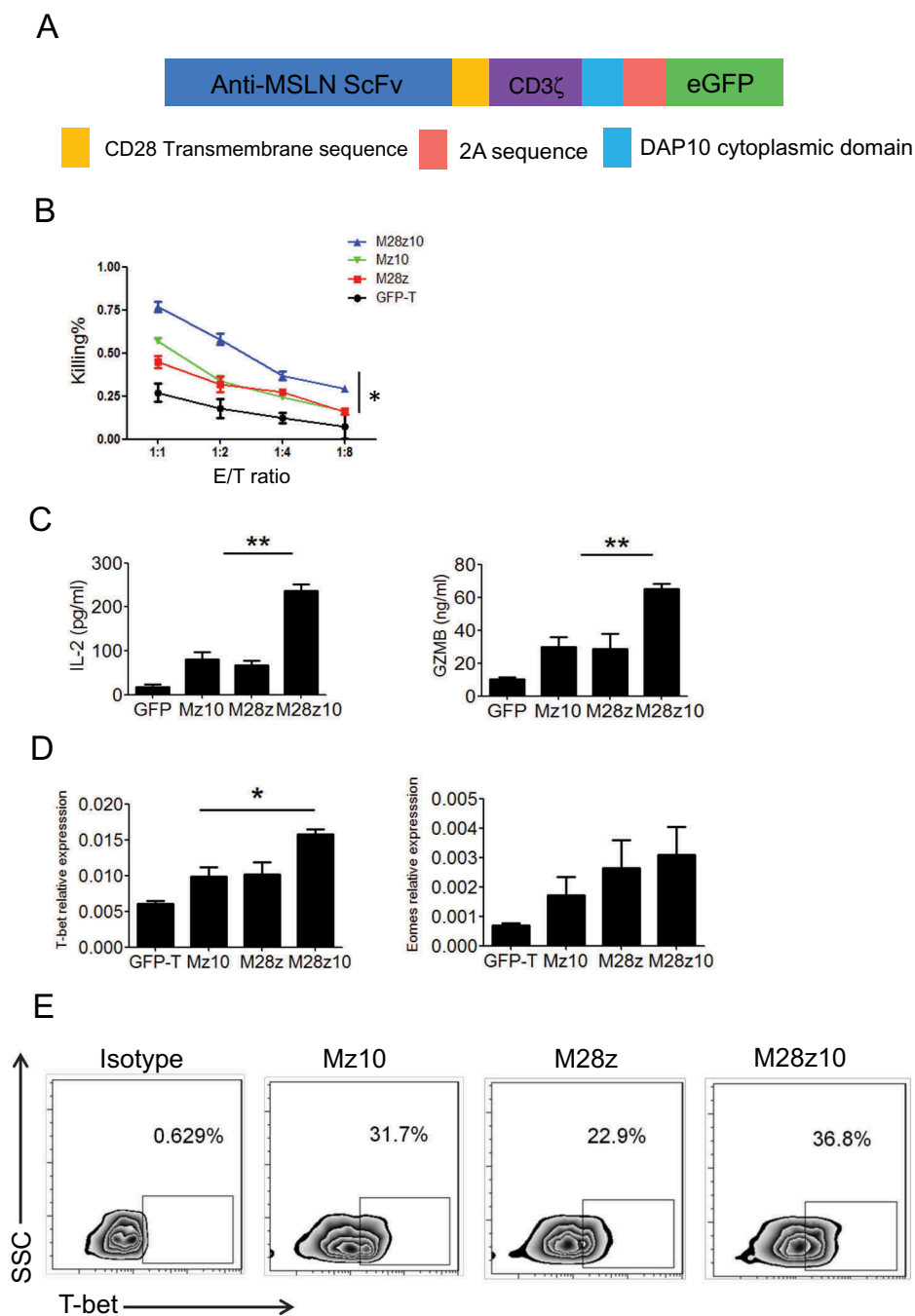


Figure 6. Synergistic effect of CD28 and DAP10 cytoplasmic domains in promoting the effector function of CAR-T cells. (A) Schematic diagram of Mz10 vector construction. (B) Eighteen-hour *in vitro* killing assay of Mz10, M28z, M28z10, and GFP T cells on the A549GL cells at each E:T ratio. (C) Detection of IL-2, granzyme B secretion by Mz10, M28z, M28z10, and GFP T cells after co-culture with A549GL cells for 18 h at E:T = 1:2. (D) Detection of T-bet and Eomes mRNA level in Mz10, M28z, M28z10, and GFP T cells after co-culture with A549GL cells at E:T = 2:1 by qRT-PCR. (E) Detection of T-bet expression in Mz10, M28z, M28z10 T cells after co-culture with A549GL cells at E:T = 2:1 for 18h by intracellular flowcytometry staining. * $P < 0.05$, ** $P < 0.01$, and *** $P < 0.001$.

and IL-15, can support NKG2D expression on immune cell.³³ These findings prompted us to ascertain the importance of activating DAP10 signaling in T cells to facilitate tumor eradication. We incorporated the DAP10 cytoplasmic domain into second-generation CAR vectors, and found the enhanced cytotoxicity and cytokine secretion by these CAR transduced human T cells. Our data is consistent with previous report demonstrating that activation of NKG2D and DAP10 can directly elicit T cell killing or enhance their cytotoxicity against target cells,^{37–39} and bystander activated memory CD8 T cells

control early pathogen load through NKG2D.⁴⁰ In contrast, silencing NKG2D and DAP10 can reduce the cytotoxicity of T and NK cell,⁴¹ and NKG2D dysfunction impairs anti-tumor activities of memory CD8 + T cell.⁴² Besides, activation of NKG2D and DAP10 also enhance the inflammatory cytokine production by murine CD8 + T cells as reported previously,^{43,44} and NKG2D signaling are also able to promote T cell infiltration and accumulation in tumors and live,^{45,46} which are consistent with our *in vivo* results obtained from lung cancer PDX mouse model.

Some pioneering studies generated chimeric NKG2D receptor T cells harboring the NKG2D extracellular domain, DAP10 and the CD3z activation domain to redirect T cells to recognize and kill tumors expressing NKG2D ligands.^{47–49} However, the effect of DAP10 incorporation had not been tested in CAR-T cells containing CD28 or 4-1BB co-stimulatory domains and targeting diverse types of TAAs. In the present study, we hypothesized that the activation of DAP10 signaling in CAR-T cells will improve anti-tumor activity. We incorporated the DAP10 cytoplasmic domain into second-generation CAR vectors and indeed found superior anti-tumor efficacy of CAR-T cells targeting TAAs including Mesothelin and Glypican 3, which is worthy being further tested in clinical trials.

Materials and methods

Chimeric antigen receptor constructs and lentivirus production

The second-generation anti-MSLN and anti-GPC3 CAR vectors were previously reported.^{20,30} The human DAP10 cytoplasmic domain sequence was obtained from the UniProt database (ID: Q9UBK5). The third-generation anti-MSLN and anti-GPC3 CARs containing the DAP10 cytoplasmic domain sequence were synthesized by Genscript (Nanjing) Co., Ltd. (Nanjing, China), and cloned into the second-generation lentiviral vector pWPXLd. Lentivirus particles were produced in HEK-293T cells after polyethyleneimine (Sigma-Aldrich, St Louis, MO, USA)-mediated transfection. HEK-293T cells were co-transduced with the pWPXLd-based lentiviral plasmid and two packaging plasmids, psPAX2 and pMD.2G. Lentivirus-containing supernatants were harvested at 48 and 72 hours post-transduction and filtered through a 0.45- μ m filter.

Isolation, transduction, and expansion of primary human T lymphocytes

Peripheral blood mononuclear cells (PBMCs) were isolated from the cord blood of healthy donors using Lymphoprep (StemCell Technologies, Canada). T cells were negatively selected from PBMCs using a MACS Pan T Cell Isolation Kit (Miltenyi Biotec, Bergisch Gladbach, Germany) and activated using microbeads coated with anti-human CD3, anti-human CD2 and anti-human CD28 antibodies (Miltenyi Biotec) at a 1:2 bead:cell ratio and a density of 2.5×10^6 cells/ml for 2 days in RPMI-1640 medium supplemented with 10% heat-inactivated fetal bovine serum (FBS), 100 IU/ml recombinant human IL-2, 10 mM HEPES, 2 mM glutamine and 1% penicillin/streptomycin. On post-activation day 2, T cells were transfected with chimeric vector lentiviral supernatants in the presence of 8 μ g/ml polybrene (Sigma-Aldrich, St Louis, USA). Twelve hours after transfection, T cells were cultured in fresh medium containing IL-2 (300 U/mL); subsequently, fresh medium was added every 2–3 days to maintain cell density within the range of $0.5\text{--}1 \times 10^6$ cells/ml. Healthy PBMC donors provided informed consent for the use of their samples for research purposes, and all procedures were approved

by the Research Ethics Board of the Guangzhou Institutes of Biomedicine and Health (GIBH).

Cells and culture conditions

HEK-293T cells were maintained in Dulbecco's modified Eagle's medium (DMEM) (Gibco, Grand Island, NY, USA). A549 (human lung adenocarcinoma), H460 (human large cell lung cancer), HepG2 (human HCC), and HC04 (human HCC) cells were maintained in RPMI-1640. DMEM and RPMI-1640 medium were supplemented with 10% heat-inactivated FBS (Gibco/Life Technologies), 10 mM HEPES, 2 mM glutamine (Gibco/Life Technologies) and 1% penicillin/streptomycin. All cells were cultured at 37°C in an atmosphere of 5% carbon dioxide.

Flow cytometry

Flow cytometry was performed on a Fortessa cytometer (BD Biosciences, San Jose, CA), and data were analyzed using FlowJo software (FlowJo, LLC, Ashland, OR, USA). The antibodies used, including anti-human CD3-APC (clone UCHT1), anti-human CD4-APC (clone OKT4), anti-human CD8-PE (clone OKT8), anti-human CD279 (PD-1)-APC (clone eBioJ105), anti-human NKG2D-APC (clone 1D11), anti-human CD25-PE (clone BC96), anti-human CD69-APC (clone FN50), anti-human CD107a-APC (clone H4A3), anti-human T-bet-percp5.5 (Clone 4B10), mouse IgG1kappa isotype control-PE and mouse IgG1kappa isotype control-APC (clone MOPC-21), were purchased from Biolegend, San Diego, CA, USA. All FACS-related staining was performed on ice for 30 minutes, and cells were then washed with PBS containing 1% FBS before cytometry analysis. Intracellular staining of T-bet was achieved with True-Nuclear™ Transcription Factor Buffer Set (Biolegend, San Diego, CA, USA). Peripheral blood (PB), spleen (SP) and tumor samples from mouse xenografts were treated with red blood cell lysis buffer (Biolegend), and the cells were stained with the corresponding antibodies.

Cytotoxicity assays

The H460GL, MSLN+ H460GL, A549GL, HepG2GL, and HC04GL target cells were incubated with GFP T cells and anti-MSLN or anti-GPC3 CAR-T cells at the indicated ratio in triplicate wells of U-bottomed 96-well plates. Target cell viability was monitored 18 hours later by adding 100 μ l/well of the substrate D-luciferin (potassium salt) (Cayman Chemical, USA) at 150 μ g/ml. Background luminescence was negligible (< 1% of the signal from wells containing only target cells). The percent viability (%) was calculated as experimental signal/maximal signal \times 100, and the percent lysis was equal to 100–percent viability.

Serial killing assays

GFP, M28z, M28z10, Mbbz, and Mbbz10 T cells were initially co-cultured with A549GL cells at an E:T ratio of 1:2 in a 96-well plate. After 24 hours, suspended T cells were transferred to another 96-well plate, and the remaining adherent cells were assayed for luminescence; then, the same number of A549GL cells was added to the T cells. After 24 hours, this procedure was repeated to achieve 3 rounds of serial killing. When the last co-

culture was finished, the culture supernatant was harvested to detect cytokine secretion by T cells.

Cytokine release assays

ELISA kits for IL-2, IFN- γ , granzyme B and GM-CSF were purchased from eBioscience, San Diego, CA, USA, and all ELISAs were performed according to the manufacturer's protocols. T cells were co-cultured with target cells at an E:T ratio of 1:2 for 18 hours. The culture supernatants were then collected and analyzed for secretion of the cytokines IL-2, IFN- γ , GM-CSF and granzyme B using ELISA kits.

Quantitative real-time PCR

mRNA was extracted from cells with TRIzol reagent (Qiagen, Stockach, Germany) and reverse-transcribed into cDNA using a PrimeScriptTM RT Reagent Kit (Takara, Japan). All reactions were performed with TransStart Tip Green qPCR SuperMix (TransGene, Beijing, China) on a Bio-Rad CFX96 Real-time PCR Machine (Bio-Rad, Hercules, CA, USA) using the following primers: human NKG2D forward, 5'-CAAGATCTTCCCTCTCTGAGCA-3', and reverse, 5'-GGCCACAGTAACTTTCGGTCA-3'; Human DAP10 forward, 5'-GCAGGGTGACATCCGCTATT-3', and reverse, 5'-GAACAAGAGCCTGAAGTGCC-3'. Human T-bet forward, 5'-CAGGGACGGCGGATGTTC-3', and reverse, 5'-TTTCCACACTGCACCCACTT-3' Human Eomes forward, 5' - GGTTCAGGTTCTGGCTTCC-3' and reverse 5'-ACATTTTGTGCCCCTGCATGT-3'.

Immunohistochemistry

Tumor tissue sections were fixed with 10% paraformaldehyde, embedded in paraffin, sectioned at a thickness of 4 μ m, and immunostained with antibodies specific for Human CD3 (OKT-3), (Biolegend, US) overnight at 4 ° C, followed by secondary staining with secondary goat anti-mouse (ZSGB-BIO, Beijing, China). Images of all sections were obtained with a microscope (DMI6000B; Leica Microsystems, Wetzlar, Germany).

Xenograft models and in vivo assessment

Animal experiments were performed in the Laboratory Animal Center of GIBH, and all animal procedures were approved by the Animal Welfare Committee of GIBH. All protocols were approved by the relevant Institutional Animal Care and Use Committee (IACUC). All mice were maintained in specific pathogen-free (SPF)-grade cages and were provided autoclaved food and water. To develop the cell line-based lung cancer xenograft models, 5×10^5 A549GL cells in 200 μ l of PBS were injected subcutaneously into the right flanks of NSI mice aged 6–8 weeks. Fifteen days after cell transplantation, the mice were divided into three groups: GFP, M28z, and M28z10. On day 15, the percentage of GFP-positive M28z and M28z10 T cells was normalized with untransduced T cells, and 5×10^6 CAR-T cells and an equivalent number of GFP T cells were injected through the tail vein into each tumor-bearing NSI mouse. Tumors were

measured every 3 days with a caliper to determine the subcutaneous growth rate.

To develop the primary lung cancer mouse models, surgical tumor samples obtained from Sun Yat-Sen University Cancer Center (Guangzhou, China) were transplanted s.c. into NSI mice. Tumors that reached approximately 1000 mm³ were removed and passed into secondary recipients for expansion for further cancer research. Tumors were cut into $2 \times 2 \times 2$ mm³ pieces and transplanted into the right flanks of NSI mice. Then, 18 days after transplantation, the mice were infused with the following groups of T cells: GFP, M28z or M28z10. The percentage of GFP-positive cells was normalized with untransduced T cells, and 5×10^6 CAR-T cells and an equivalent number of GFP T cells were injected i.v. into each mouse. Tumors were measured every 3 days with a caliper. The tumor volume was calculated using the following equation: (length \times width²)/2.

To develop the primary human HCC mouse models, surgical tumor samples obtained from Sun Yat-Sen University Cancer Center (Guangzhou, China) were transplanted s.c. into NSI mice. Tumors that reached approximately 1000 mm³ were removed and passed into secondary recipients for expansion for further cancer research. Tumors were cut into $2 \times 2 \times 2$ mm³ pieces and transplanted into the right flanks of NSI mice. Then, 15 days after transplantation, the mice were infused with the following groups of T cells: GFP, G28z and G28z10. The percentage of GFP-positive cells was normalized with untransduced T cells, and 5×10^6 CAR-T cells and an equivalent number of GFP T cells were injected i.v. into each mouse. Tumors were measured every 3 days with a caliper. The tumor volume was calculated using the following equation: (length \times width²)/2.

Statistics

The data are presented as the mean \pm standard error of the means (s.e.m.). Unpaired Student's t-tests (two-tailed) were used to determine the statistical significance of differences between samples, and $P < 0.05$ indicated statistical significance. All statistical analyses were performed using Prism software, version 5.0 (GraphPad, Inc., San Diego, CA, USA).

Funding

This paper/achievement is supported by National Natural Science Foundation of China (NSFC) - 81522002, 81773301; The Strategic Priority Research Program of the Chinese Academy of Sciences, Grant No. XDB19030205, No. XDA12050305; The Natural Science Fund of Guangdong Province: Distinguished Young Scholars (Grant No.: 2014A030306028), Doctoral Foundation (Grant No.: 2017A030310381) The National Major Scientific and Technological Special Project for "Significant New Drugs Development" (Grant No.: SQ2018ZX090201), The Guangdong Provincial Applied Science and Technology Research & Development Program (Grant No.: 2016B020237006), The Frontier and key technology innovation special grant from the Department of Science and Technology of Guangdong province, (2015B020227003), (2014B020225005), (2016B030229006).

Notes on contributor

Rucong Zhao, Lin Cheng and Zhiwu Jiang contributed to the conception and design, collection and/or assembly of data, data analysis and interpretation and manuscript writing. Xinru Wei, Zhiwu Jiang contributed to the provision of study material or patients, collection and/or

assembly of data. Baiheng Li, Simiao Lin, Suna Wang and Qiting Wu provided animal care and administrative supports. Yao Yao and Duanqing Pei contributed to the conception and design and provided financial support. Xuchao Zhang, Yilong Wu, Xin Du, Pentao Liu, Yangqiu Li, Shuzhong Cui contributed to the conception and design. Rucong Zhao and Pentao Liu contributed to the conception and design, data analysis and interpretation, manuscript writing, and final approval of manuscript and provided financial support. All authors read and approved the final manuscript.

ORCID

Lin Cheng  <http://orcid.org/0000-0001-7180-0388>
 Pentao Liu  <http://orcid.org/0000-0001-5774-9678>
 Yangqiu Li  <http://orcid.org/0000-0002-0974-4036>

References

- Grupp SA, Kalos M, Barrett D, Aplenc R, Porter DL, Rheingold SR, Teachey DT, Chew A, Hauck B, Wright JF, Chimeric antigen receptor-modified T cells for acute lymphoid leukemia. *N Engl J Med.* 2013;368(16):1509–1518. doi:10.1056/NEJMoa1215134.
- Kalos M, Levine BL, Porter DL, Katz S, Grupp SA, Bagg A, June CH. T Cells with Chimeric Antigen Receptors Have Potent Antitumor Effects and Can Establish Memory in Patients with Advanced Leukemia. *Science Translational Medicine.* 2011;3(95):95ra73.
- Maude SL, Frey N, Shaw PA, Aplenc R, Barrett DM, Bunin NJ, Chew A, Gonzalez VE, Zheng ZH, Lacey SF, et al. Chimeric Antigen Receptor T Cells for Sustained Remissions in Leukemia. *New England Journal of Medicine.* 2014;371(16):1507–1517. doi:10.1056/NEJMoa1407222.
- Liu B, Song Y, Liu D. Clinical trials of CAR-T cells in China. *J Hematol Oncol.* 2017;10(1):166. doi:10.1186/s13045-017-0535-7.
- Liu J, Zhong JF, Zhang X, Zhang C. Allogeneic CD19-CAR-T cell infusion after allogeneic hematopoietic stem cell transplantation in B cell malignancies. *J Hematol Oncol.* 2017;10(1):35. doi:10.1186/s13045-017-0405-3.
- Dotti G, Gottschalk S, Savoldo B, Brenner MK. Design and development of therapies using chimeric antigen receptor-expressing T cells. *Immunological Reviews.* 2014;257(1):107–126. doi:10.1111/immr.12131.
- Jena B, Dotti G, Cooper L. Redirecting T-cell specificity by introducing a tumor-specific chimeric antigen receptor. *Blood.* 2010;116(7):1035–1044. doi:10.1182/blood-2010-01-043737.
- Zhang E, Xu H. A new insight in chimeric antigen receptor-engineered T cells for cancer immunotherapy. *J Hematol Oncol.* 2017;10(1):1. doi:10.1186/s13045-016-0379-6.
- Kowolik CM, Topp MS, Gonzalez S, Pfeiffer T, Olivares S, Gonzalez N, Smith DD, Forman SJ, Jensen MC, Cooper L. CD28 costimulation provided through a CD19-specific chimeric antigen receptor enhances in vivo persistence and antitumor efficacy of adoptively transferred T cells. *Cancer Research.* 2006;66(22):10995–11004. doi:10.1158/0008-5472.CAN-06-0160.
- Song DG, Ye QR, Carpenito C, Poussin M, Wang LP, Ji CY, Figini M, June CH, Coukos G, Powell DJ. In Vivo Persistence, Tumor Localization, and Antitumor Activity of CAR-Engineered T Cells Is Enhanced by Costimulatory Signaling through CD137 (4-1BB). *Cancer Research.* 2011;71(13):4617–4627. doi:10.1158/0008-5472.CAN-11-0422.
- Beatty GL, Moon EK. Chimeric antigen receptor T cells are vulnerable to immunosuppressive mechanisms present within the tumor microenvironment. *Oncoimmunology.* 2014;3(11):e970027.
- Mirzaei HR, Rodriguez A, Shepphird J, Brown CE, Badie B. Chimeric Antigen Receptors T Cell Therapy in Solid Tumor: challenges and Clinical Applications. *Frontiers in Immunology.* 2017;8.
- Yu S, Li A, Liu Q, Li T, Yuan X, Han X, Wu K. Chimeric antigen receptor T cells: a novel therapy for solid tumors. *J Hematol Oncol.* 2017;10(1):78. doi:10.1186/s13045-017-0444-9.
- Gargett T, Brown MP. Different cytokine and stimulation conditions influence the expansion and immune phenotype of third-generation chimeric antigen receptor T cells specific for tumor antigen GD2. *Cytotherapy.* 2015;17(4):487–495. doi:10.1016/j.jcyt.2014.12.002.
- Enblad G, Karlsson H, Wikstrom KI, Essand M, Savoldo B, Brenner MK, Dotti G, Hoglund M, Hagberg H, Loskog A. *CD19-targeting third generation CAR T cells for relapsed and refractory lymphoma and leukemia - report from the Swedish phase Ulla trial.* *Cancer Immunology Research.* 2016. 4(1).
- Guedan S, Chen X, Madar A, Carpenito C, McGettigan SE, Frigault MJ, Lee J, Posey AD, Scholler J, Scholler N, et al. ICOS-based chimeric antigen receptors program bipolar T(H)17/T(H)1 cells. *Blood.* 2014;124(7):1070–1080. doi:10.1182/blood-2013-10-535245.
- Foster AE, Mahendravada A, Shinnars NP, Chang WC, Crisostomo J, Lu A, Khalil M, Morschl E, Shaw JL, Saha S, et al. Regulated Expansion and Survival of Chimeric Antigen Receptor-Modified T Cells Using Small Molecule-Dependent Inducible MyD88/CD40. *Molecular Therapy.* 2017;25(9):2176–2188. doi:10.1016/j.ymthe.2017.06.014.
- Hombach AA, Heiders J, Foppe M, Chmielewski M, Abken H. OX40 costimulation by a chimeric antigen receptor abrogates CD28 and IL-2 induced IL-10 secretion by redirected CD4(+) T cells. *Oncoimmunology.* 2012;1(4). doi:10.4161/onci.19855.
- Song DG, Powell DJ. Pro-survival signaling via CD27 costimulation drives effective CAR T-cell therapy. *Oncoimmunology.* 2012;1(4):doi:10.4161/onci.19458.
- Lai Y, Weng J, Wei X, Qin L, Lai P, Zhao R, Jiang Z, Li B, Lin S, Wang S, et al. Toll-like receptor 2 costimulation potentiates the antitumor efficacy of CAR T Cells. *Leukemia.* 2018;32(3):801–808.
- Bauer S, Groh V, Wu J, Steinle A, Phillips JH, Lanier LL, Spies T. Activation of NK cells and T cells by NKG2D, a receptor for stress-inducible MICA. *Science.* 1999;285(5428):727–729.
- Lanier LL. NKG2D Receptor and Its Ligands in Host Defense. *Cancer Immunology Research.* 2015;3(6):575–582. doi:10.1158/2326-6066.CIR-15-0098.
- Prajapati K, Perez C, Rojas LBP, Burke B, Guevara-Patino JA. Functions of NKG2D in CD8(+) T cells: an opportunity for immunotherapy. *Cell Mol Immunol.* 2018. doi:10.1038/cmi.2017.161.
- Lanier LL. NKG2D Receptor and Its Ligands in Host Defense. *Cancer Immunol Res.* 2015;3(6):575–582. doi:10.1158/2326-6066.CIR-15-0098.
- Ye W, Jiang Z, Li GX, Xiao Y, Lin S, Lai Y, Wang S, Li B, Jia B, Li Y, et al. Quantitative evaluation of the immunodeficiency of a mouse strain by tumor engraftments. *J Hematol Oncol.* 2015;8:59. doi:10.1186/s13045-015-0156-y.
- Wei X, Lai Y, Li J, Qin L, Xu Y, Zhao R, Li B, Lin S, Wang S, Wu Q, et al. PSCA and MUC1 in non-small-cell lung cancer as targets of chimeric antigen receptor T cells. *Oncoimmunology.* 2017;6(3):e1284722. doi:10.1080/2162402X.2017.1284722.
- Capurro M, Wanless IR, Sherman M, Deboer G, Shi W, Miyoshi E, Filmus J. Glypican-3: A novel serum and histochemical marker for hepatocellular carcinoma. *Gastroenterology.* 2003;125(1):89–97.
- Nakatsura T, Yoshitake Y, Senju S, Monji M, Komori H, Motomura Y, Hosaka S, Beppu T, Ishiko T, Kamohara H, et al. Glypican-3, overexpressed specifically in human hepatocellular carcinoma, is a novel tumor marker. *Biochemical and Biophysical Research Communications.* 2003;306(1):16–25.
- Zhai B, Shi DH, Gao HP, Qi XX, Jiang H, Zhang Y, Chi JC, Ruan HY, Wang HM, Ru QHC, et al. A phase I study of anti-GPC3 chimeric antigen receptor modified T cells (GPC3 CAR-T) in Chinese patients with refractory or relapsed GPC3+hepatocellular carcinoma (r/r GPC3+HCC). *Journal of Clinical Oncology.* 2017;35(15):3049 (Meeting Abstract).
- Jiang Z, Jiang X, Chen S, Lai Y, Wei X, Li B, Lin S, Wang S, Wu Q, Liang Q, et al. Anti-GPC3-CAR T Cells Suppress the Growth of Tumor Cells in Patient-Derived Xenografts of Hepatocellular Carcinoma. *Frontiers in Immunology.* 2016;7:690.

31. Lazarevic V, Glimcher LH, Lord GM. T-bet: a bridge between innate and adaptive immunity. *Nat Rev Immunol.* 2013;13(11):777–789. doi:10.1038/nri3536.
32. Raveney BJ, Oki S, Hohjoh H, Nakamura M, Sato W, Murata M, Yamamura T. Eomesodermin-expressing T-helper cells are essential for chronic neuroinflammation. *Nat Commun.* 2015;6:8437. doi:10.1038/ncomms9437.
33. Lopez-Soto A, Huergo-Zapico L, Acebes-Huerta A, Villa-Alvarez M, Gonzalez S. NKG2D signaling in cancer immunosurveillance. *International Journal of Cancer.* 2015;136(8):1741–1750. doi:10.1002/ijc.28775.
34. Mincheva-Nilsson L, Baranov V. Cancer exosomes and NKG2D receptor-ligand interactions: impairing NKG2D-mediated cytotoxicity and anti-tumour immune surveillance. *Seminars in Cancer Biology.* 2014;28:24–30. doi:10.1016/j.semcancer.2014.02.010.
35. Groh V, Wu J, Yee C, Spies T. Tumour-derived soluble MIC ligands impair expression of NKG2D and T-cell activation. *Nature.* 2002;419(6908):734–738. doi:10.1038/nature01112.
36. Lundholm M, Schroder M, Nagaeva O, Baranov V, Widmark A, Mincheva-Nilsson L, Wikstrom P. Prostate Tumor-Derived Exosomes Down-Regulate NKG2D Expression on Natural Killer Cells and CD8(+) T Cells: mechanism of Immune Evasion. *Plos One.* 2014;9(9):e10892.
37. Verneris MR, Karimi M, Baker J, Jayaswal A, Negrin RS. Role of NKG2D signaling in the cytotoxicity of activated and expanded CD8+ T cells. *Blood.* 2004;103(8):3065–3072. doi:10.1182/blood-2003-06-2125.
38. Walsh KB, Lanier LL, Lane TE. NKG2D receptor signaling enhances cytolytic activity by virus-specific CD8+ T cells: evidence for a protective role in virus-induced encephalitis. *J Virol.* 2008;82(6):3031–3044. doi:10.1128/JVI.02033-07.
39. Markiewicz MA, Wise EL, Buchwald ZS, Pinto AK, Zafirova B, Polic B, Shaw AS. RAE1epsilon ligand expressed on pancreatic islets recruits NKG2D receptor-expressing cytotoxic T cells independent of T cell receptor recognition. *Immunity.* 2012;36(1):132–141. doi:10.1016/j.immuni.2011.11.014.
40. Chu T, Tyznik AJ, Roepke S, Berkley AM, Woodward-Davis A, Pattacini L, Bevan MJ, Zehn D, Prlic M. Bystander-activated memory CD8 T cells control early pathogen load in an innate-like, NKG2D-dependent manner. *Cell Rep.* 2013;3(3):701–708. doi:10.1016/j.celrep.2013.02.020.
41. Karimi M, Cao TM, Baker JA, Verneris MR, Soares L, Negrin RS. Silencing human NKG2D, DAP10, and DAP12 reduces cytotoxicity of activated CD8+ T cells and NK cells. *J Immunol.* 2005;175(12):7819–7828.
42. Andre MC, Sigurdardottir D, Kuttruff S, Pommerl B, Handgretinger R, Rammensee HG, Steinle A. Impaired tumor rejection by memory CD8 T cells in mice with NKG2D dysfunction. *Int J Cancer.* 2012;131(7):1601–1610. doi:10.1002/ijc.26191.
43. Whitman E, Barber A. NKG2D receptor activation of NF-kappaB enhances inflammatory cytokine production in murine effector CD8(+) T cells. *Mol Immunol.* 2015;63(2):268–278. doi:10.1016/j.molimm.2014.07.015.
44. Kavazovic I, Lenartic M, Jelencic V, Jurkovic S, Lemmermann NAW, Jonjic S, Polic B, Wensveen FM. NKG2D stimulation of CD8(+) T cells during priming promotes their capacity to produce cytokines in response to viral infection in mice. *European Journal of Immunology.* 2017;47(7):1123–1135. doi:10.1002/eji.201646805.
45. Huang WC, Easom NJ, Tang XZ, Gill US, Singh H, Robertson F, Chang C, Trowsdale J, Davidson BR, Rosenberg WM, et al. T Cells Infiltrating Diseased Liver Express Ligands for the NKG2D Stress Surveillance System. *J Immunol.* 2017;198(3):1172–1182. doi:10.4049/jimmunol.1601313.
46. Hu J, Zhu S, Xia X, Zhang L, Kleinerman ES, Li S. CD8+T cell-specific induction of NKG2D receptor by doxorubicin plus interleukin-12 and its contribution to CD8+T cell accumulation in tumors. *Mol Cancer.* 2014;13:34. doi:10.1186/1476-4598-13-34.
47. Barber A, Zhang T, DeMars LR, Conejo-Garcia J, Roby KF, Sentman CL. Chimeric NKG2D receptor-bearing T cells as immunotherapy for ovarian cancer. *Cancer Research.* 2007;67(10):5003–5008. doi:10.1158/0008-5472.CAN-06-4047.
48. Barber A, Zhang T, Megli CJ, Wu JL, Meehan KR, Sentman CL. Chimeric NKG2D receptor-expressing T cells as an immunotherapy for multiple myeloma. *Experimental Hematology.* 2008;36(10):1318–1328. doi:10.1016/j.exphem.2008.04.010.
49. Zhang T, Barber A, Sentman CL. Generation of antitumor responses by genetic modification of primary human T cells with a chimeric NKG2D receptor. *Cancer Research.* 2006;66(11):5927–5933. doi:10.1158/0008-5472.CAN-06-0130.